Effect of Recrystallization on the Molecular Mobility of a Copolymer of Vinylidene Fluoride and Hexafluoropropylene

Valentin V. Kochervinskij,[1] Inna A. Malyshkina,[2] Natalia P. Bessonova,[1] Sergey N. Suljanov,[3] Kirill A. Dembo[3]

[1]*Karpov Institute of Physical Chemistry, State Research Center of the Russian Federation, Vorontsovo Pole 10, Moscow 103064, Russia*
[2]*Physical Faculty, M. V. Lomonosov Moscow State University, Leninskie Gory, Moscow 119991, Russia*
[3]*Institute of Crystallography, Russian Academy of Sciences, Leninsky Prospekt 53, Moscow 119333, Russia*

Received 27 February 2010; accepted 24 June 2010
DOI 10.1002/app.32993
Published online 6 October 2010 in Wiley Online Library (wileyonlinelibrary.com).

ABSTRACT: Relaxation processes in copolymers of vinylidene fluoride with hexafluoropropylene (93/7) were studied by means of a dielectric method. The initial extruded film was recrystallized by free heating to temperatures above the melting point and by subsequent cooling. This increased both the perfection of the crystal phase and the degree of crystallinity. The impact of recrystallization on both the relaxation times (τ's) and the activation parameters of the local mobility (β process) and micro-Brownian cooperative mobility in amorphous phase (α_a process) was almost negligible, whereas the τ's of the α_c relaxation were an order of magnitude higher after recrystallization. Qualitatively, it was predicted by the soliton model for the α_c relaxation. The recrystallization affected characteristics of the transition at the highest temperature (α) registered in the region of the melting of the crystals even more. The process is related to the relaxation of the space charge formed by ionogenic impurities, which migrate through the amorphous phase with high free volume. It was shown that the dynamics in the amorphous phase controlled the drift mobility of free charge carriers and, by that, determined the τ of the space charge relaxation process. The structuring processes during the recrystallization also affected the parameters of the order–disorder transition in the low-perfect ferroelectric (antiferroelectric) phase. © 2010 Wiley Periodicals, Inc. J Appl Polym Sci 120: 13–20, 2011

Key words: dielectric properties; ferroelectricity; fluoropolymers; relaxation

INTRODUCTION

Poly(vinylidene fluoride) (PVDF) and its copolymers are of great interest of researchers because of the variety of their properties valuable for applications. It is one of the crystallizing polymers possessing ferroelectricity.[1,2] Strong piezoelectric activity and pyroactivity in these compounds along with the specific properties of the polymers allow one to obtain a variety of sensors whose characteristics cannot be obtained with classical inorganic materials.[3,4] Fluorinated elastomers based on this class of polymers were recently applied to membrane production engineering, where they can be used as a matrix in gel polymer electrolytes.[5] The conductivity (σ) in these systems is controlled by the structural and dynamic characteristics of the polymer, and thus, the study of molecular mobility in these polymers is a topical problem.

The relaxation processes in two copolymers of vinylidene fluoride (VDF) with hexafluoropropylene (HFP) were investigated earlier by means of broadband dielectric spectroscopy.[6] Three or four relaxation transitions were detected, depending on the composition of the copolymers. In this study, the effects of recrystallization on the molecular mobility in a VDF/HFP 93/7 copolymer were investigated. We found that increased perfection of the crystalline structure weakly influenced both the local and cooperative micro-Brownian dynamics. At the same time, the essential effect on the α_c relaxation related to the crystalline phase was observed. The high-temperature relaxation process caused by melting also appeared to be sensitive to the structurization at recrystallization.

EXPERIMENTAL

VDF/HFP 93/7 copolymers (Plast-Polymer, St. Petersburg, Russia), with their composition controlled by ^{19}F-NMR,[7] were investigated. The initial films were prepared by extrusion. Recrystallization was made by the free heating of the film above its melting point with subsequent cooling.

Dielectric measurements were performed with a Novocontrol (Novocontrol GmbH, Hundsangen, Germany) Concept 40 broadband dielectric spectrometer at 10^{-1} to 10^{7} Hz and -100 to 150°C.

Correspondence to: V. V. Kochervinskij (kochval@mail.ru).

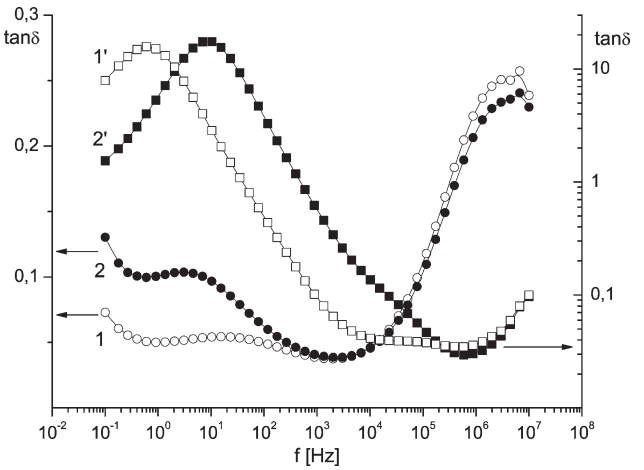

Figure 1 F dependence on the loss tangent [tan δ(f)] illustrating the processes of (1,2) αa and αc and (1′,2′) α relaxation at (1,2) 20 and (1′,2′) 100°C: (1,1′) the initial sample and (2,2′) the recrystallized sample.

Differential scanning calorimetry (DSC) was carried out with a PerkinElmer DSK-7 calorimeter (Waltham, Massachusetts, USA). The heating rate was 20°/min, and the sample weights were about 20 mg. Calibration was made with indium. Wide-angle X-ray scattering (WAXS) measurements were performed in the transition mode with KARD-6 and KARD-7 X-ray diffractometers (Institute of Crystallography RAS, Moscow, Russia)[8] with two-dimensional area position-sensitive detectors [Cu Kα radiation, wavelength (λ) = 0.154 nm]. The diffraction peaks were analyzed by profile fitting.

RESULTS

Figure 1 demonstrates the changes in several relaxation processes observed both in the initial and recrystallized films. According to ref. 6, the four relaxation transitions in the initial film were denoted as β, α_a, α_c, and α in the order of increasing temperature [or decreasing frequency (*f*)]. Three of these transitions (α_a, α_c, and α) are shown at the dielectric loss tangent [tan δ(*f*)] spectra presented in Figure 1. The α_a and α_c relaxations overlapped. Their separation was made with the assumption that both relaxations were described by the Havriliak–Negami function:

$$\varepsilon^*(\omega) - \varepsilon_\infty = \sum_k \frac{\Delta\varepsilon_k}{\left[1 + (i\omega\tau_k)^{1-a_k}\right]^{b_k}} - iA\omega^{-s} \qquad (1)$$

ε* is the complex dielectric permittivity, ω is the angular frequency (ω = 2*π**f*), *i* is the imaginary unit, where the first term on the right express the dielectric relaxation based on Havriliak–Negami function, where Δε (= $\varepsilon_0 - \varepsilon_\infty$) is the relaxation strength [where ε_0 and ε_∞ are the low-*f* and high-*f* limits of the real part of the permittivity (ε′)], τ is the relaxation time, and both *a* and *b* ($0 < a, b \leq 1$) are parameters expressing the asymmetry and width of the distribution of τ's. The subscript *k* is used to express multiple relaxation processes (in our case, *k* = 2). The second term on the right expresses the contribution from the direct-current conductivity (σ_{dc}), where *A* is the constant and *s* ($s \leq 1$) is the power parameter.[9] Figure 2 shows an example of the curve-fitting with regard to the imaginary part of the dielectric permittivity [ε″(ω)] obtained for both the initial and recrystallized films at 20°C.

The temperature behavior of the relaxation transitions mentioned previously for both the initial and recrystallized samples was demonstrated on a correlation diagram in Arrhenius coordinates (Fig. 3). The β, α_c, and α transitions followed the Arrhenius equation:

$$f = f_0 \exp\left(-\frac{E_a}{kT}\right) \qquad (2)$$

where f_0 is a constant, *k* is the Boltzmann constant, E_a is the activation energy, and *T* is the temperature.

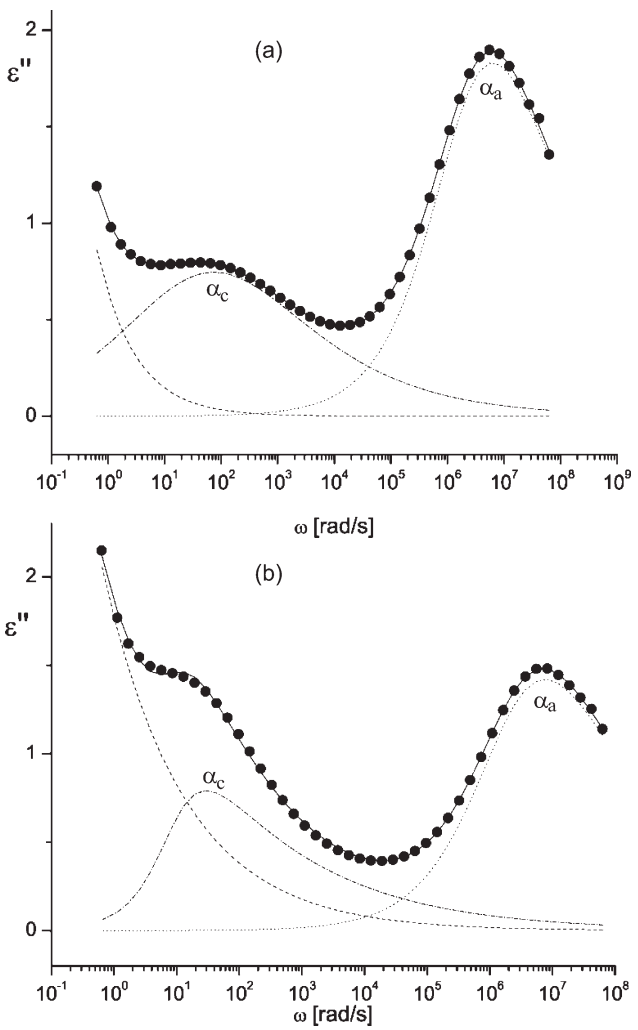

Figure 2 Decomposition of the dielectric loss spectra [ε″(ω)] of the (a) initial and (b) recrystallized samples of the VDF/HFP copolymer at 20°C into the α_a and α_c processes and σ according to eq. (1).

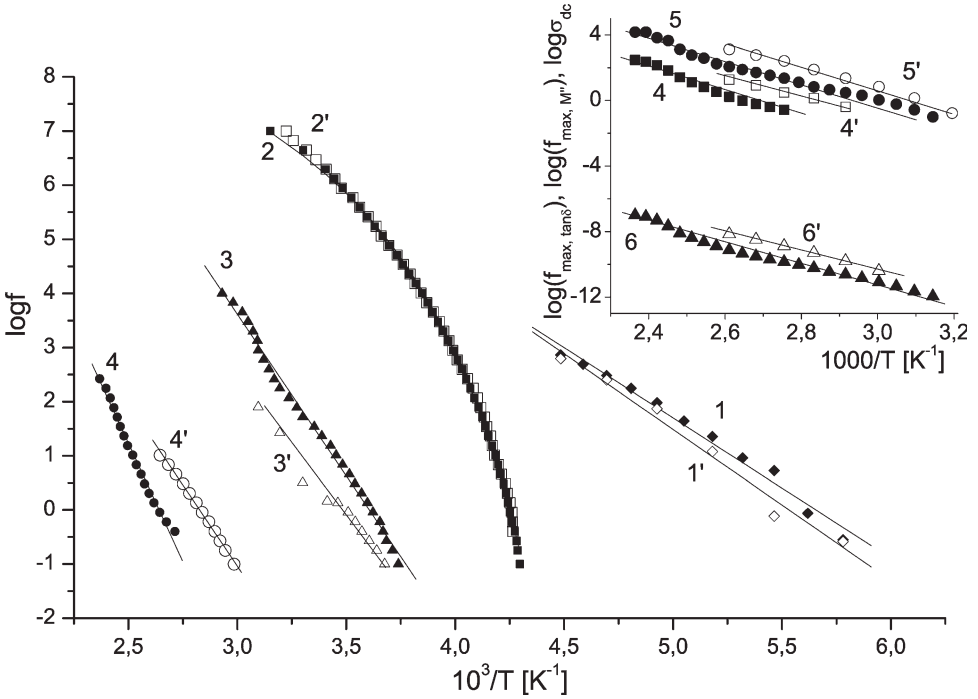

Figure 3 Correlation diagrams for the processes of (1,1′) β, (2,2′) α_a, (3,3′) α_c, and (4,4′,5,5′,6,6′) α relaxation in the (1–6) initial and (1′–6′) recrystallized VDF/HFP 93/7 films. The insert shows additional data on the α process: (4,4′) tan δ(*f*) peaks, (5,5′) peaks of the imaginary part of the dielectric modulus [$M''(f)$], and (6,6′) σ_{dc}.

α_a processes followed not Arrhenius but the Vogel–Tamman–Fulcher (VTF)[10] equation

$$f = f_0 \exp\left(-\frac{B}{T - T_0}\right) \tag{3}$$

where f_0 and B are the fit parameters and T_0 is the characteristic temperature, which is usually approximately 50° lower than the glass-transition temperature (T_g).

For the α_a transition, the conventional glass-transition temperature (T'), for which the reorientation f of the kinetic units was 1 Hz, was obtained from curves 2 and 2′ in Figure 2. Also, the thermodynamic parameter (m; the fragility),[11] which characterizes the changes of cooperativity with temperature, was calculated with eq. (4):

$$m = \frac{d\log\tau}{d\left(T'/T\right)} = \frac{B}{T' \times \ln 10 \times \left(1 - \frac{T_0}{T'}\right)^2} \tag{4}$$

All of these parameters for all types of mobility are summarized in Table I.

As shown, the influence of recrystallization on the β τ's and processes was weak, whereas for the high-temperature processes (α_c and α), it was much stronger. We discuss these facts from the point of view of the structural modifications controlled by DSC and WAXS. DSC scans (Fig. 4) showed that the width of the melting peak was reduced after recrystallization, whereas the peak temperature remained approximately the same. It is known that the width of the endothermic peak and the crystal size (l_c) distribution are related in crystalline polymers, so this

TABLE I
E_a, Parameters of VTF Analysis [T_0, B, and log f_0 from eq. (3)], ΔS, T', and m for the Relaxation Processes in the Initial and Recrystallized Films of the VDF/HFP 93/7 Copolymers

Sample	Initial film				Recrystallized film			
Relaxation process	β	α_a	α_c	α	β	α_a	α_c	α
T_0 (K)	—	199 ± 2	—	—	—	195 ± 1	—	—
B	—	845 ± 33	—	—	—	980 ± 45	—	—
log f_0	—	10.3 ± 0.3	—	—	—	10.6 ± 0.2	—	—
E_a (kJ/mol)	48 ± 2	78 ± 3	114 ± 3	155 ± 4	52 ± 2	66 ± 2	101 ± 4	106 ± 2
ΔS (J/mol K)	38 ± 2	146 ± 7	174 ± 8	169 ± 8	54 ± 3	93 ± 5	116 ± 5	59 ± 5
T' (K)	177 ± 5	235 ± 5	278 ± 5	379 ± 5	181 ± 5	234 ± 5	286 ± 5	355 ± 5
m	—	65 ± 3	—	—	—	71 ± 3	—	—

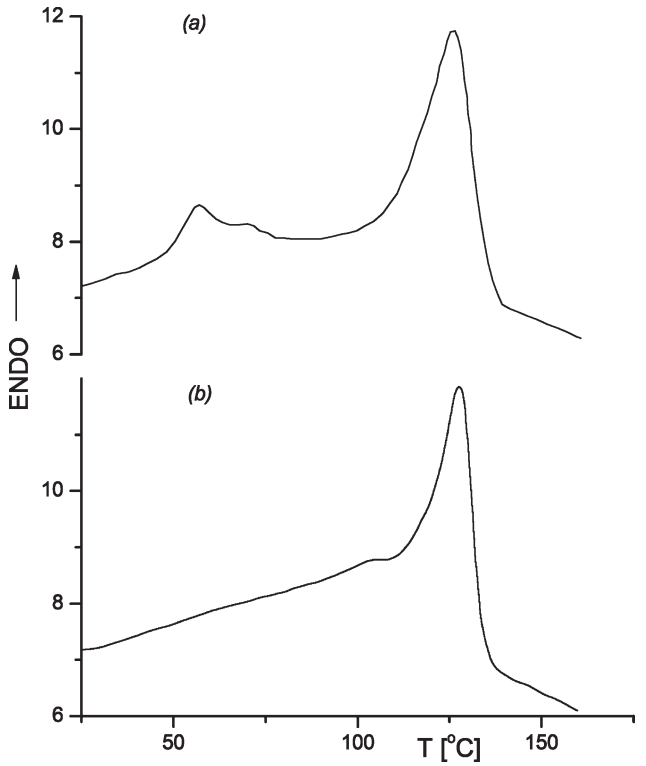

Figure 4 DSC thermograms for the (a) initial and (b) recrystallized VDF/HFP films.

distribution was more narrow in the recrystallized sample. The shape of the peak at the low-temperature side pointed to the fact that the fraction of the small (defective) crystals decreased after recrystallization. It was equivalent to the growth of their mean size. This was confirmed by WAXS measurements (Fig. 5). l_c was estimated by the Scherrer formula:

$$l_c = \frac{0.9\lambda}{\cos\theta\sqrt{\beta^2 - \beta_r{}^2}} \quad (5)$$

where θ is the diffraction angle, β and β_r are the half-widths of the analyzed and reference lines. According to Table II, the l_c values in different lattice directions were larger in the recrystallized film. We could also judge the structural perfection of the film by the increase of the number of peaks typical for the α phase. Intramolecular peaks indicated the process of the structural perfection of the lattice.

The crystallinity (ϕ) was calculated for both films by decomposition of the experimental curves into peak components and the amorphous halo (Table II). ϕ increased from 0.30 to 0.38 after recrystallization. Figure 4 shows more information about the changes in the crystal structure after recrystallization. In addition to the melting peak, two endothermic peaks at lower temperatures were observed in the initial film. The peak at the lowest temperature was related to the order–disorder phase transition in the low-perfect (QL-) ferroelectric phase.[6] Only one endothermic process was left after recrystallization, and it shifted to higher temperatures. A similar effect was observed in PVDF,[12,13] where the low-temperature endotherm was not observed in the second heating cycle. Detailed experiments demonstrated[11] that the low-temperature endotherm was related to the process of melting in the QL- crystals formed as the result of the secondary crystallization. We adhere to the same opinion.

DISCUSSION

Here, we begin to discuss the influence of the recrystallization on the relaxation processes in VDF/HFP from the data on α_a transition. According to our results, $\Delta\varepsilon$ for the α_a transition decreased in the entire temperature interval after recrystallization. Because ϕ was higher in this sample (Table I), this process was related to the amorphous phase and/or to its interphase boundaries with a crystal.[14,15]

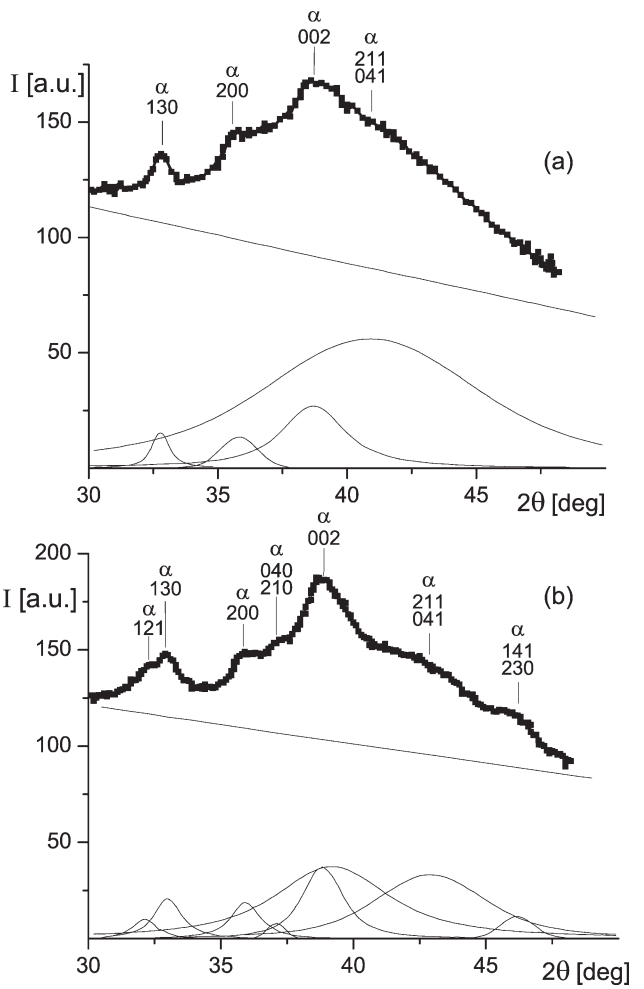

Figure 5 Wide-angle X-ray diffraction patterns in the region of intramolecular order manifestation for the (a) initial and (b) recrystallized VDF/HFP films. I is the intensity of the diffraction.

TABLE II
Structural Parameters of the VDF/HFP 93/7 Films Before and After Recrystallization

Sample	l_{002} (nm)	l_{200} (nm)	l_{021} (nm)	l_{100} (nm)	ϕ
Initial film	3.0 ± 0.2	5.1 ± 0.3	3.2 ± 0.2	2.6 ± 0.1	0.30 ± 0.02
Recrystallized film	4.5 ± 0.2	6.6 ± 0.3	3.6 ± 0.2	3.4 ± 0.2	0.38 ± 0.02

We also wanted to check possible relations between the relaxation parameters of the α_a and α_c transitions. For this, the temperature dependences of the mean relaxation time (τ_0; Fig. 6) were compared in the region of temperatures where the specified relaxation processes overlapped. Those processes were separated according to the procedure shown in Figure 2. We assumed that for temperatures above 30°C, $\tau(T)$ for the α_a transition followed Arrhenius behavior, and therefore, E_a and the activation entropy (ΔS) were calculated for this process [Fig. 6(a)]. Their values are also listed in Table I. Recrystallization was accompanied by a decrease in the activation parameters, and ΔS decreased more essentially. The observed difference was related to the modifications in the crystalline polymers at annealing.[16] It is known that the latter leads to the formation of more perfect crystals because of the displacement of chemical defects into the interlamellar intervals. We considered the comonomer component with CF_3 groups as a chemical defect, which got into the crystal and broke its perfection.[6] We considered HFP groups as branchings with respect to the PVDF chains, and so their displacement into the amorphous phase should have decreased the packing density of the latter.[17] Thus, the interlamellar intervals in the recrystallized sample should have contained raised concentration of both the CF_3 groups and other branchings, end groups, and head-head-tail-tail (HHTT) defects. Lower packing density in the amorphous phase obviously was the main reason for the changes in m, E_a, and ΔS (Table II).

As shown in Figures 3 and 6(b), recrystallization also affected the α_c relaxation. The τ's of this process were almost 10 times higher in the recrystallized sample. In PVDF crystallized in a nonpolar α-modification, this relaxation mechanism is usually connected with the longitudinal component of the dipole moment, which can change its direction to the opposite at conformational transformations of the $TGTG^- \leftrightarrow G^-TGT$ (T goes for trans, G goes for gauche) type.[18] Because the copolymer under study crystallized in the same modification,[6] we proceeded from the same relaxation mechanism. We assumed the mobility of conformational defect along the c axis of a crystal, and thus, τ should have depended on the crystal's longitudinal size. The last was estimated with the width of the 002 peak, which was broader in the initial sample (Fig. 5). Thus, if we proceeded from the α_c relaxation mechanism proposed in refs. 18–21, τ should have been higher in the recrystallized sample, which is what we observed, as shown in Figures 3 and 6(b).

As shown in Table I, there was a drop in the E_a value for this process in the recrystallized sample. The reason for it, in our opinion, was in the nature of α_a mobility. According to ref. 18, the stage of initiation of the initial conformational defect in a crystal is an important and required part of the relaxation mobility in the α phase. This defect may originate from a specific structure of interphase boundaries in crystalline polymers. It is theoretically predicted that there can be a layer with an intermediate form of order.[22,23] Because of the chain molecular structure, the same molecule can be located both in the crystal and in the transition layer (amorphous phase). Consider that the mobility at the α_a transition takes place in this interlayer,[14,15] and the reorientation f's of the segments involved in the cooperative mobility reach 10^6–10^7 Hz (see Figs. 3 and 6) at

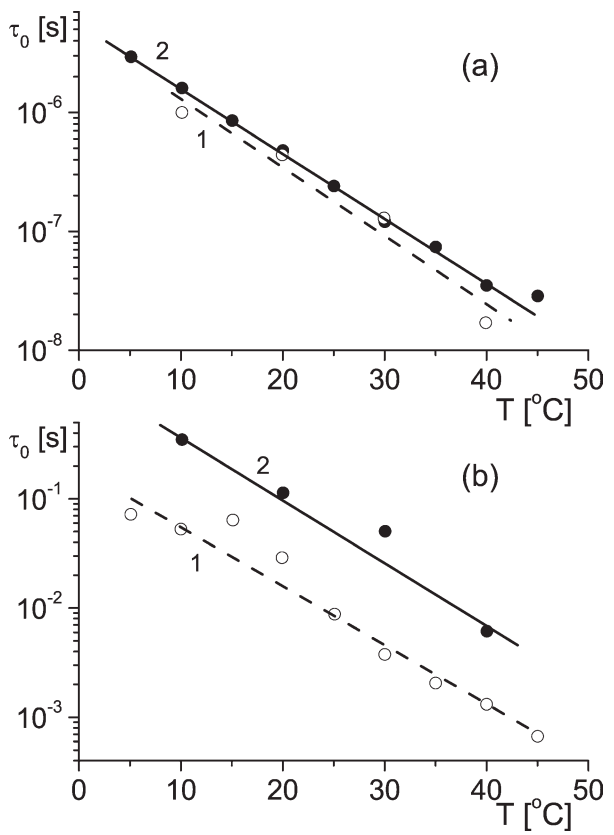

Figure 6 Temperature dependence of τ_0 for the (a) α_a and (b) α_c processes for the (1) initial and (2) recrystallized VDF/HFP films.

temperatures when the mobility in the crystal appears. Because the adjacent segments of the same chain at the crystal surface and in the interface layer are covalently bound, the high amplitude cooperative motions of the chains in the interface layer will cause internal stress for the chain in the crystal. Such internal stress, along with thermal fluctuations, can be the origin for the conformational defect in the crystal. The higher the reorientation f of segments in the interface region is, the higher the probability of appearance of the conformational defect will be.

As follows from Table I, the E_a and ΔS values for the α_a transition at temperatures above 30°C were lower in the recrystallized sample. This may have been the reason why the reorientation f's of the segments in the transition zone appeared to be higher in the recrystallized sample [Figs. 3 and 6(a)]. This meant that the enhanced internal stress for the chains at the crystal interfaces generated conformational defects inside the crystal. This should have decreased the E_a and ΔS values for the α_c relaxation, as observed in the experiment (Table I).

If the α_c relaxation is limited by the formation of the conformational defect in the crystal, it becomes clear why there is a quantitative disagreement between the longitudinal length of the crystal (l_{002}) and the τ of the α_c transition. As follows from Table II, there was a 50% change in l_c after recrystallization. However, at the same time, τ changed by a factor of 10. When the conformational defect moves along the macromolecule axis by the solitone mechanism,[24,25] the macroscopic τ will not be limited by the high propagation speed of the solitone wave. Because there is a displacement of chemical defects and impurities into the interlamellar intervals at recrystallization, the probability of solitone wave attenuation at its propagation from one crystal to another should increase.[26] This should result in an additional increase of the macroscopic τ, as shown in the experiment.

Let us discuss the effect of recrystallization on the dielectric anomalies, which we connected earlier to the diffusive order–disorder transition in the QL-ferroelectric or antiferroelectric phase.[6,27] Figure 7 illustrates that there was a dielectric anomaly at approximately 60°C for the initial film, which is typical for the diffusive ferroelectric phase transition. This conclusion was supported by the existence of the endothermic peak (Fig. 4). As noted previously, the last was assigned to the melting of the secondary crystals. Before the first measurement cycle, the initial film was kept at room temperature for several years, and slow processes of secondary crystallization[11] should have been completed here. In the second measurement cycle (recrystallized film), the low-temperature endotherm broadened and shifted to higher temperatures (Fig. 4), and so did the

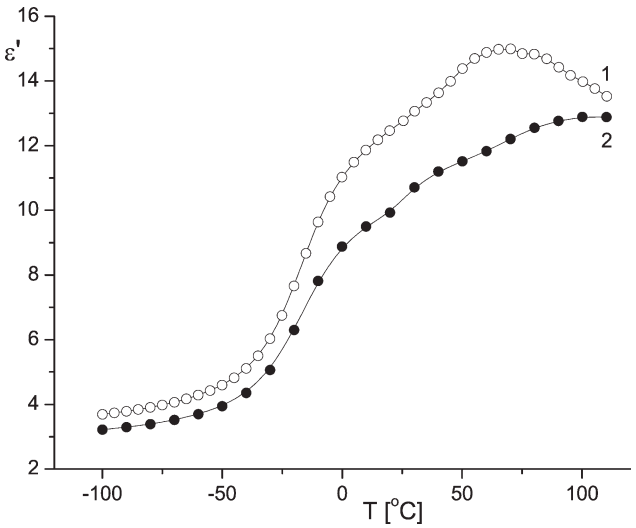

Figure 7 Temperature dependence of the dielectric permittivity (ε') for the (1) initial and (2) recrystallized VDF/HFP films at $f = 1$ kHz.

dielectric anomaly (Fig. 7). The shift of this anomaly to higher temperatures in the recrystallized film is typical for ferroelectric materials in general and for polymer ferroelectrics in particular. It is known that the increase in l_c both in inorganic ferroelectric crystals[28] and polymer ferroelectrics[28,29] is accompanied by a shift of the Curie point to higher temperatures. In our case, we related the QL- ferroelectric (antiferroelectric) phase areas to the 100 peak.[27] It follows from Table II that the size of the coherent scattering region for this peak appeared to be higher for the recrystallized film. This should have led to the shift of the transition to higher temperatures, as confirmed by the experiment (see Fig. 7). The smaller diffusiveness of the phase transition in the initial film was attributed to the fact that spontaneous polarization areas in the QL- or antiferroelectric phase were partially activated by the orientation processes emerging at the extrusion.[27] Nonreversible conformational changes[27] and a partial loss of the mean orientation registered by the magnitude of the birefringence[7] took place in the initial film during the first heating cycle. It was directly demonstrated that the decrease in the mean orientation was accompanied by the appropriate increase in the diffusiveness of the observed phase transition. Thus, the formation of spontaneous polarization regions in the QL- ferroelectric (antiferroelectric) phase was limited by the processes of the secondary crystallization. The last may have led to the formation of small and imperfect crystals where the spontaneous polarization regions may have been localized. A similar conclusion was drawn in ref. 12 from another type of experiment.

Let us now discuss the high-temperature α relaxation, which we related to the manifestation of the

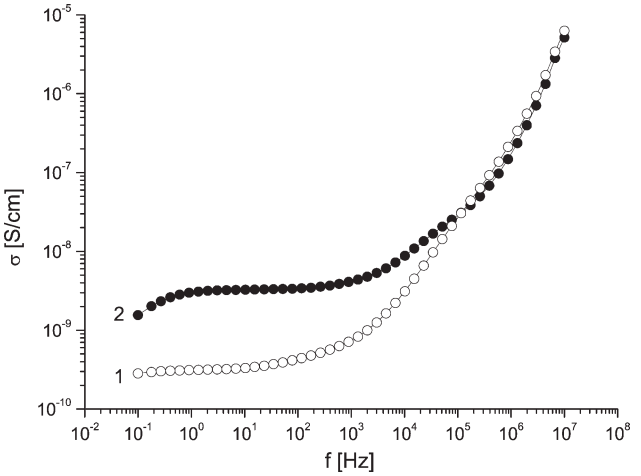

Figure 8 Alternating-current conductivity [σ(*f*)] spectra for the (1) initial and (2) recrystallized VDF/HFP films at 100°C.

space charge. As shown in Figures 1 and 3, the transition shifted to higher *f*'s and its E_a decreased after recrystallization (Table I). This should have been related to the modification of the microscopic structure of the amorphous phase. If we proceed from the Maxwell–Wagner–Scillars relaxation and take into account the heterogeneity of the two phases, at first approximation

$$\tau = \frac{\varepsilon_a \varepsilon_0}{A\sigma} \tag{6}$$

where ε_0 is the free space permittivity and ε_a is the dielectric permittivity of the matrix containing the volume fraction of inclusions with σ and the form factor *A*. It follows from eq. (6) that if this relaxation mechanism is realized for the α relaxation, the experimentally detected decrease of τ (Fig. 3) for the recrystallized sample should be accompanied, for example, by the growth of σ in one of the phases. As shown in Figure 8, the plateau value of σ increased. As shown in the insert in Figure 3(6,6′), this was valid for all temperature regions of this relaxation. Moreover, there was a certain quantitative correspondence. The σ changed by an order of magnitude (Fig. 8), and so did τ after recrystallization (Fig. 3).

We now discuss the changes in the electrical parameters, taking into account the structural modifications at recrystallization. As noted, this process was accompanied by the displacement of chemical defects (including the copolymer CF_3 groups) into interlamellar amorphous intervals. The less dense (because of stronger steric interactions of CF_3 groups) amorphous phase played a special role in the mechanisms of space charge carrier mobility. In such a heterogeneous system, extrinsic charge carriers will migrate through areas with increased free volume. As we speak about extrinsic conduction in dielectrics, the charges can be trapped in the local sites generated by various defects. The particular feature of the observed systems was that the phase where charge carriers moved was in a liquidlike state where the atoms and molecules had intensive micro-Brownian dynamics, so charge carriers moved under multiple trapping–detrapping mechanisms. The number of such events in time units specified the drift mobility of the charges. Thus, the last was obviously determined by the *f*'s and the amplitudes of the reorientation of kinetic units in the amorphous phase.

As noted previously, the activation parameters of such mobility (α_a process) appeared to be lower in the recrystallized sample (Table I), and so the corresponding *f*'s of the reorientation of segments in the amorphous phase (at temperatures of the α transition) were higher in this sample (Fig. 3). Such increase meant the enhancement of the space charge carriers' mobility. With the assumption that there was the same type and same concentration of the charges in both samples, this should have led to an increase in σ after recrystallization, as was observed in the experiment (Fig. 8).

CONCLUSIONS

During the process of recrystallization taking place in the extruded VDF/HFP 93/7 film at free heating, more perfect crystals of the α phase were formed, and φ increased. This was due to the changes in the microstructure of interlamellar intervals: they became less closely packed because of the displaced chemical defects of macromolecules, including the CF_3 groups of the HFP monomer. So the probability of the appearance of conformational defects became lower, which led to an increase in the τ's of mobility in the crystal phase. At the same time, the mobility of the charge carriers, which formed the space charge, increased, and the corresponding τ decreased.

References

1. Ferroelectric Polymers—Chemistry, Physics and Applications; Nalva, H. S., Ed.; Marcel Dekker: New York, 1995.
2. Kochervinskii, V. V. Russ Chem Rev 1999, 68, 821.
3. The Application of Ferroelectric Polymers; Wang, T. T., Herbert, J. M., Glass, A. M., Eds.; Blackie: Glasgow, 1988.
4. Kochervinskii, V. V. Russ Chem Rev 1994, 63, 367.
5. Xiao, Q.; Zhou, X. Acta Polym Sinica 2003, 2, 139.
6. Kochervinskii, V. V.; Malyshkina, I. A.; Markin, G. V.; Gavrilova, N. D.; Bessonova, N. P. J Appl Polym Sci 2007, 105, 1101.
7. Kochervinskii, V. V. Polym Sci Ser A 1998, 40, 1020.
8. Sulyanov, S. N.; Popov, A. N.; Kheiker, D. M. J Appl Crystallogr 1994, 27, 934.
9. Hofmann, A.; Kremer, F.; Schoenhals, A.; Fischer, E. W. In Disorder Effects on Relaxational Processes; Richert, R., Blumen, A., Eds.; Springer: Berlin, 1994; p 309.

10. Donth, E. Relaxation and Thermodynamics in Polymers: Glass Transition; Akademie: Berlin, 1992.
11. Neidhofer, M.; Beaume, F.; Ibos, L.; Bernes, A.; Lacabanne, C. Polymer 2004, 45, 1679.
12. Kochervinskii, V.; Malyshkina, I.; Gavrilova, N.; Sulyanov, S.; Bessonova, N. J Non-Cryst Solids 2007, 353, 4443.
13. Hahn, B.; Wendorff, J. H.; Yoon, D. Y. Macromolecules 1985, 18, 718.
14. Hahn, B.; Herrmann-Schonher, O.; Wendorff, J. H. Polymer 1987, 28, 201.
15. Zuza, E.; Ugartemendia, J. M.; Lopez, A.; Meaurio, E.; Lejardi, A.; Sarasua, J.-R. Polymer 2008, 49, 4427.
16. Yeh, G. S.; Hosemann, R.; Loboda-Cackovic, Y.; Cackovic, H. Polymer 1976, 17, 309.
17. Dlubek, G.; Stein, J.; Lupke, T.; Bamford, D.; Petters, K.; Hubner, C.; Alam, M. A.; Hill, J. J Polym Sci Part B: Polym Phys 2002, 40, 65.
18. Miamoto, Y.; Miyaji, H.; Asai, K. J Polym Sci Polym Phys Ed 1980, 18, 597.
19. Takahashi, Y.; Miyaji, K. Macromolecules 1983, 16, 1789.
20. Carbeck, J. D.; Rutledge, G. C. Macromolecules 1996, 29, 5190.
21. Mowry, S. W.; Rutledge, G. C. Macromolecules 2002, 35, 4539.
22. Flory, P. J.; Yoon, D. Y.; Dill, K. A. Macromolecules 1984, 17, 862.
23. Yoon, D. Y.; Flory, P. J. Macromolecules 1984, 17, 868.
24. Skinner, J. L.; Park, Y. H. Macromolecules 1984, 17, 1735.
25. Zubova, E. A.; Balabanov, N. K.; Manevich, L. I. Polymer 2004, 48, 1802.
26. Kochervinsky, V. V. Polym Sci Ser C 2006, 48, 38.
27. Kochervinskii, V.; Kozlova, N.; Khnykov, A.; Shcherbina, M.; Sulyanov, S.; Dembo, K. J Appl Polym Sci 2010, 116, 695.
28. Kochervinsky, V. V. Polym Sci Ser B 2005, 47, 75.
29. Tashiro, K.; Tanaka, R.; Ushitora, K.; Kobayashi, M. Ferroelectrics 1995, 171, 145.